

## ARTICLE OPEN



# An effective way to control the radical reaction and its mechanism in EPDM under $\gamma$ -ray irradiation

Yiyang Zhou<sup>1,2</sup>, Qiuyue Meng<sup>1,2</sup>, Ming Chen<sup>1,2</sup>, Chenxi Wang<sup>1,2</sup>, Tao Jiang<sup>2,3</sup>, Jingsong Zhou<sup>1,2</sup>, Ping Wang<sup>4</sup>, Lei Xia<sup>5</sup>, Yezi You<sup>5</sup>, Haibing Wei<sup>1,2</sup> and Yunsheng Ding<sup>1,2</sup>✉

The effects of a compound that contains a xanthate group named DIP on the radical reactions and structural evolution of the ethylene propylene diene monomer (EPDM) were investigated. It was found that the structural evolution and long-term stability of the EPDM can be realized by controlling the radical reaction in the matrixes of EPDM during  $\gamma$ -ray irradiation. The results show that the DIP can prevent EPDM deterioration, when the  $\gamma$ -ray irradiation dose reaches 450 kGy, the retention rate of the elongation at break and tensile strength of the EPDM samples containing 1 wt% DIP could remain about 90% and 160%, while those of additive-free EPDM are only about 33% and 70%. On the other hand, the thermal stability of the EPDM samples decreases markedly with the dose increasing under  $\gamma$ -ray irradiation. However, the thermal decomposition temperature of the EPDM samples containing DIP remains basically unchanged after irradiation, and DIP can also improve the oxidation resistance of the EPDM. Electron spin resonance studies reveal that DIP can effectively control the radical reactions inside the EPDM during  $\gamma$ -ray irradiation. Rheology results show that the structural evolution of the EPDM can be well controlled under  $\gamma$ -ray irradiation owing to the presence of DIP in the EPDM matrixes. Density functional theory calculations indicate that the reversible radical reactions inside EPDM/DIP systems are crucial in realizing the long-term stability and controllable structural evolution of the EPDM under  $\gamma$ -ray irradiation.

*npj Materials Degradation* (2023)7:17; <https://doi.org/10.1038/s41529-023-00334-9>

## INTRODUCTION

Expanding access to energy while at the same time drastically reducing the emissions of greenhouse gases that cause global warming and climate change is among the central challenges that humankind is confronted by in the 21<sup>st</sup> century. If no urgent action is taken to mitigate the greenhouse gas emissions, some parts of the world will be almost uninhabitable for humans by the end of this century<sup>1–3</sup>. Nuclear technologies could help the world to move away from hydrocarbon fossil fuels and speed up the transition to cleaner sources of power; in particular, nuclear power is considered to be a key technology to realize a clean-energy future<sup>4,5</sup>. However, since the Fukushima nuclear accident, the international community has put forward new and stricter requirements for the safety of nuclear power plants. Polymer-based materials are widely used in important systems of nuclear power plants, such as their low-voltage cable systems, and play a crucial role in the safe operation of nuclear facilities. However, when these materials are exposed to high-energy irradiation in the nuclear power plants, such as  $\gamma$ -ray irradiation, crosslinking and chain scission simultaneously occur inside the polymers owing to the formation of radicals caused by high-energy irradiation. This may lead to performance degradation of the materials and a huge risk associated with the operation of nuclear power plants<sup>6–8</sup>. It is thus necessary to control the radical reactions inside the polymer materials used in nuclear power plants, which might improve the operational safety of nuclear power plants and provide a firm foundation for the sustainable development of human societies.

To improve the service life of polymer-based materials, the radicals inside the polymer matrixes should be effectively

annihilated; traditional antioxidants, such as hindered phenolic compounds, are considered to be the most efficient approach for delaying the aging process of polymer materials as they can scavenge the O- or C-centered free radicals formed in polymer materials. Thus, the addition of antioxidants might improve the stability of polymers<sup>9–16</sup>. Although traditional antioxidants have been effectively used in scavenging the radicals and improving the service life of polymer materials, they would be consumed while annihilating free radicals. Indeed, Gardette et al. have reported that antioxidants are rapidly consumed under  $\gamma$ -ray irradiation<sup>17</sup>. Thus, it is important to establish a new method to realize the long-term regulation of the radical reactions and the controllable structural evolution of the polymer materials, but thus far this has remained challenging.

It is well known that thiocarbonylthio compounds are effective in controlling the radical reactions, and they are widely used in several circumstances that require the ability to control the radical reactions, such as radical polymerization<sup>18–21</sup>. Thiocarbonylthio compounds can react with free radicals and then regenerate via reversible-addition-fragmentation chain transfer, so that they can maintain the ability to control radicals during the radical polymerization process; more importantly, polymers with controlled architectures can be obtained owing to the well-controlled radical reactions in the polymerization process<sup>22–24</sup>. The above characteristics endow thiocarbonylthio compounds with a great potential in realizing the long-term stability and controllable structural evolution of the ethylene propylene diene monomer (EPDM) under  $\gamma$ -ray irradiation. However, most of the thiocarbonylthio compounds are expensive and sensitive to oxygen, which might limit their use in the stabilization of polymer materials

<sup>1</sup>School of Chemistry and Chemical Engineering, Hefei University of Technology, Hefei 230009, China. <sup>2</sup>Anhui Key Laboratory of Advanced Functional Materials and Devices, Hefei 230009, China. <sup>3</sup>School of Resources and Environmental Engineering, Hefei University of Technology, Hefei 230009, China. <sup>4</sup>School of Materials and Chemical Engineering, Anhui Jianzhu University, Hefei 230601, China. <sup>5</sup>CAS Key Laboratory of Soft Matter Chemistry, Department of Polymer Science and Engineering, University of Science and Technology of China, Hefei 230026, China. ✉email: dingys@hfut.edu.cn

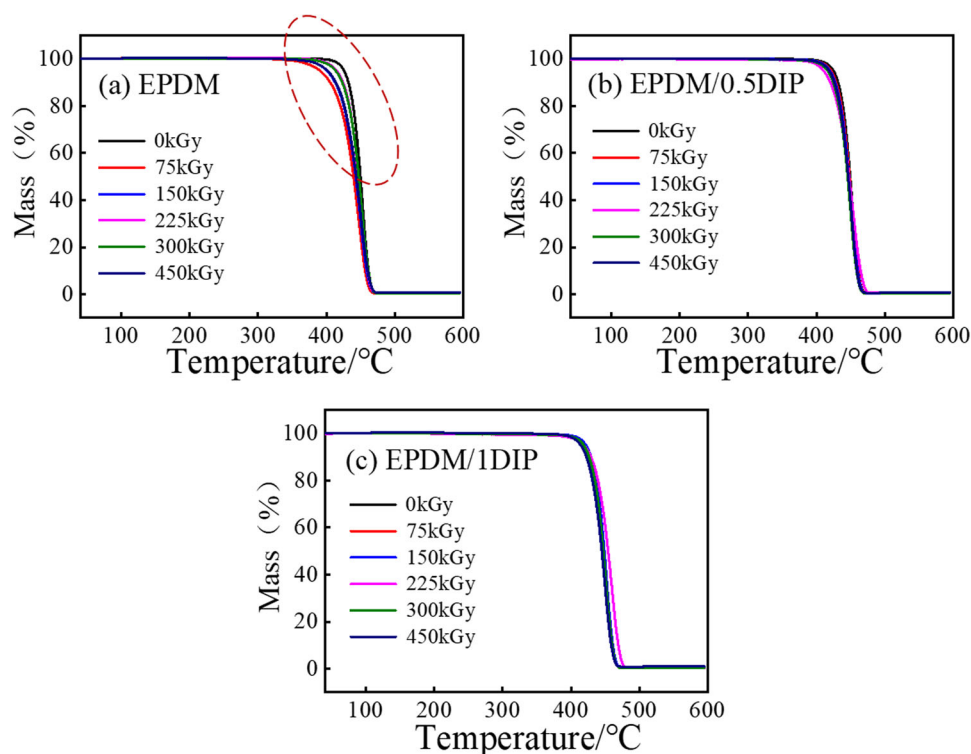


**Fig. 1** TGA curves of the EPDM and EPDM/DIP blends at different  $\gamma$ -irradiation doses. **a** EPDM, **b** EPDM/0.5DIP blend, **c** EPDM/1DIP blend.

under  $\gamma$ -ray irradiation<sup>25–28</sup>. It has been reported that xanthates ( $Z=O$ -alkyl) possess a high oxidation resistance and are unexpensive; they are thus promising candidates for use as thiocarbonylthio compounds<sup>29,30</sup>. Hence, xanthates have a strong potential in realizing the stabilization and structural conversion of polymers and revealing the effect of well-controlled radical reactions on the structural evolution of polymers under  $\gamma$ -ray irradiation.

In this work, we present a compound that contains a xanthate group named DIP, which has the ability to control the radical reactions and the conversion of radicals inside polymer matrixes. The EPDM was selected as the polymer matrix as it is often used in the electric cables of nuclear power plants<sup>31–34</sup>. We introduced DIP into the EPDM matrixes, and the effects of DIP on the radical reactions and structural conversion of the EPDM were investigated. We hypothesize that if DIP can be used to control the radical reactions in the EPDM, the introduction of compounds containing groups that are able to control the radical reactions will constitute a new strategy to control the radical reactions inside polymers and prolong their service life in harsh environments.

## RESULTS

### Thermogravimetric analysis (TGA) measurements

To examine whether DIP can stabilize the EPDM, the thermal degradation behavior of the blends and the additive-free EPDM was studied using TGA since the thermal decomposition behavior of polymers depends strongly on their microstructure<sup>35–37</sup>. The results are shown in Fig. 1, and the relevant data are presented in Table 1. After  $\gamma$ -ray irradiation, significant changes in the thermal degradation behavior are observed in the EPDM for different irradiation doses, and the thermal stability of the EPDM decreases considerably after irradiation. Although a crosslinked network is formed inside the EPDM during  $\gamma$ -ray irradiation, the poor controllability of the radical reactions induced by  $\gamma$ -ray irradiation also causes the EPDM chain to easily undergo chain scission or other reactions, such as free-radical branching reactions, which

**Table 1.** TG data of the samples with different blend compositions subjected to different  $\gamma$ -irradiation doses.

Sample	Irradiation dose/kGy	$T_{\text{onset}}$ /°C	$T_{\text{max}}$ /°C
EPDM	0	436.2	452.2
	75	419.4	446.9
	150	424.1	449.6
	225	433.6	447.1
	300	427.7	456.2
	450	424.1	449.8
EPDM/0.5DIP	0	435.5	452.4
	75	434.0	451.6
	150	432.8	451.3
	225	428.4	452.4
	300	430.9	449.0
	450	431.9	451.0
EPDM/1DIP	0	435.8	452.2
	75	434.1	450.5
	150	434.5	451.4
	225	436.9	460.2
	300	432.6	450.5
	450	428.9	449.1

seriously damage the overall EPDM microstructure; thus, the thermal stability of the unmodified EPDM decreases significantly after irradiation. It should be pointed out that the continued uncontrolled reactions between the radicals inside the EPDM as the irradiation dose increases also cause unexpected changes to the EPDM microstructure. Thus, it is found that the thermal decomposition behavior of the EPDM is dose dependent. Different from the EPDM, the change in the thermal stability of the EPDM/

DIP blends is negligible during  $\gamma$ -ray irradiation. This is because DIP can effectively control the radical reactions induced by  $\gamma$ -ray irradiation; hence, the uncontrolled structural evolution of the EPDM is significantly inhibited, resulting in the high thermal stability of the EPDM under  $\gamma$ -ray irradiation.

#### Attenuated total reflection Fourier transform infrared (ATR FT-IR) measurements

ATR FT-IR spectroscopy was employed to evaluate the effect of DIP on preventing the oxidation of the EPDM induced by the free-radical reactions, as shown in the spectrum in Fig. 2. It can be seen for the additive-free EPDM that the poor controllability of the radical reactions in the matrixes causes the EPDM chain radicals to easily react with other radicals or oxygen, which leads to the rapid generation of oxidation products inside the EPDM. The peak at around  $1712\text{ cm}^{-1}$  that can be clearly observed in the ATR FT-IR spectrum as the irradiation dose reaches 225 kGy is a powerful proof of the occurrence of reactions between the radicals and oxygen<sup>38,39</sup>. For the EPDM/DIP blends, the peaks of the oxidation products cannot easily be detected in the ATR FT-IR spectrum until the irradiation dose reaches 450 kGy. This indicates that DIP can control the free-radical reactions in the EPDM matrixes effectively; thus, the random free-radical reactions between the EPDM chain radicals and other radicals or oxygen inside the EPDM matrixes are clearly hindered, resulting in the stability of the structure and properties of the EPDM under  $\gamma$ -ray irradiation.

#### Mechanical measurements and gel content measurements

The mechanical properties and the retention of the mechanical properties after  $\gamma$ -ray irradiation are important to evaluate the irradiation resistance properties of polymer materials. The variation in the gel content and mechanical properties of the EPDM and EPDM/DIP blends at different irradiation doses is shown in Fig. 3. It can be readily seen that the gel content of all samples

increases as the absorbed dose increases, which indicates the formation of crosslinked structures induced by  $\gamma$ -ray irradiation. The introduction of DIP can significantly reduce the crosslinking degree of the EPDM: When the irradiation dose is 75 kGy, the gel content of the EPDM is 18.9%, while the gel contents of the EPDM/0.5DIP and EPDM/1DIP blends are only 7.7% and 6.7%, respectively. As the irradiation dose increases, the gel contents of the EPDM/DIP systems are still lower than that of the EPDM. In particular, when the DIP content reaches 1 wt%, the gel content of the samples is much lower than that of the additive-free EPDM until the irradiation dose reaches 450 kGy; this is because the crosslinking reaction can be inhibited by DIP inside the EPDM matrixes.

For the additive-free EPDM, the best comprehensive mechanical properties are obtained when the irradiation dose is 150 kGy owing to the formation of a crosslinked network. As the irradiation dose increases further, even if the crosslinking degree of the EPDM also increases, the performance of the EPDM is significantly reduced. The reason for this phenomenon might be that the formation of an irregular network in the EPDM owing to the uncontrollable radical reactions under a high irradiation dose, which contains a number of weakened zones, can lead to crack initiation and a significant degradation of the mechanical properties of the EPDM<sup>40</sup>. Interestingly, when the irradiation dose reaches 300 kGy, although the crosslinking degrees of the EPDM/0.5DIP and EPDM/1DIP blends are much lower than that of the EPDM, the well-controlled radical reactions inside the EPDM can lead to the formation of a regular and compact structure, which significantly enhances the mechanical properties of the EPDM/1DIP blend. Thus, the EPDM/1DIP samples can maintain an excellent performance when the irradiation dose reaches 300 kGy. The reason for the above phenomenon is that DIP can control the radicals and regenerate via reversible chain transfer; thus, the microstructural damage caused to the EPDM is effectively inhibited under  $\gamma$ -ray irradiation. Additionally, a good control of

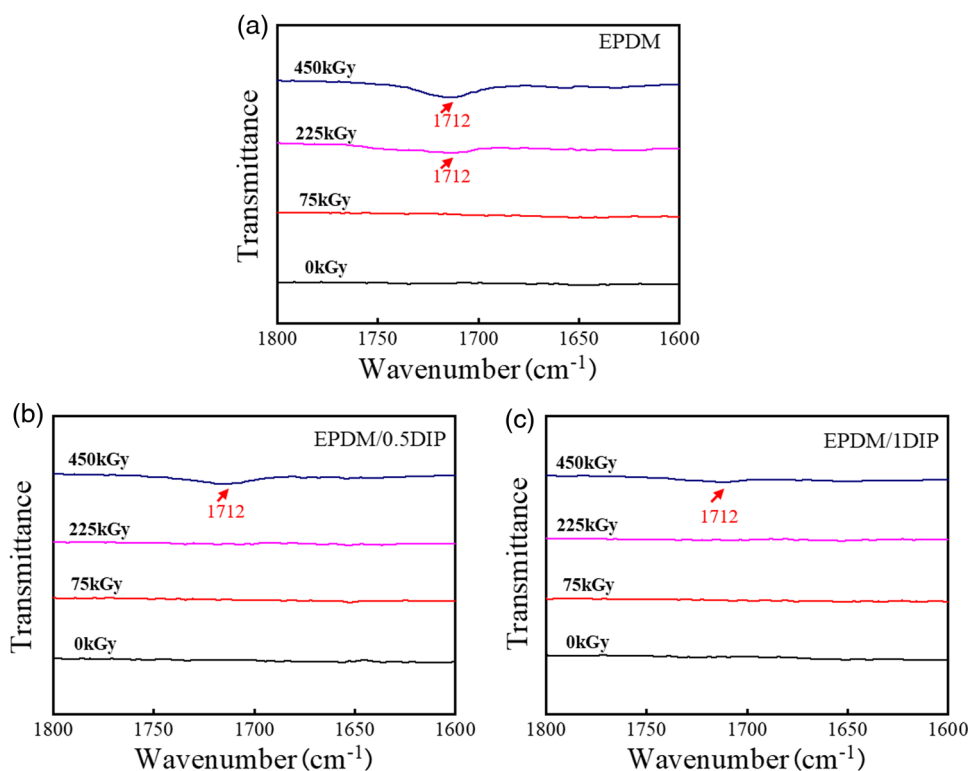


**Fig. 2** ATR FT-IR spectra of the EPDM and EPDM/DIP blends at different  $\gamma$ -irradiation doses. **a** EPDM, **b** EPDM/0.5DIP blend, **c** EPDM/1DIP blend.

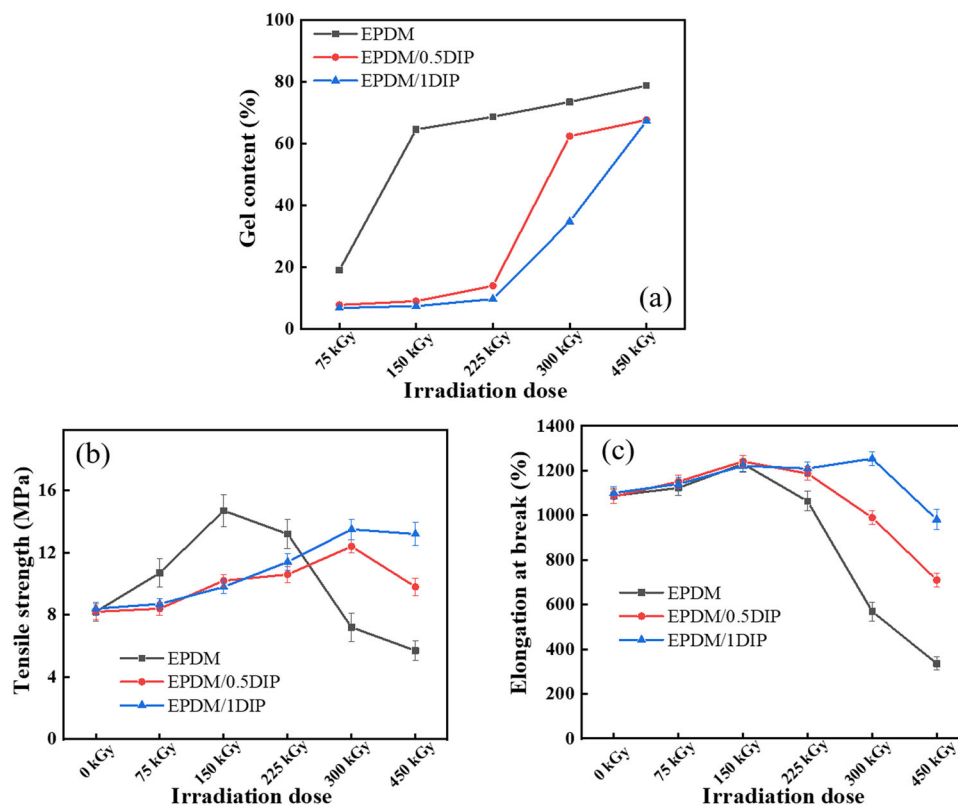


**Fig. 3** Gel fractions and mechanical properties of the EPDM and EPDM/DIP blends at different  $\gamma$ -irradiation doses. **a** Gel fractions of the EPDM and EPDM/DIP blends, **b** tensile strength of the EPDM and EPDM/DIP blends, **c** elongation at break of the EPDM and EPDM/DIP blends (Error bars stand for the standard deviations from at least five independent samples).

the structural evolution of the EPDM is realized owing to the well-controlled radical reactions in the EPDM/DIP systems. The fact that DIP can be used to achieve the long-term control of the radical reactions inside the EPDM owing to the reversible chain transfer reactions can be further proved according to the difference in the gel content between the EPDM/DIP and EPDM/antioxidant samples (Fig. S2).

To verify our hypothesis that DIP possesses the ability to control the radical reactions inside the EPDM, room-temperature ESR measurements were performed to detect the active radicals of the EPDM before and after  $\gamma$ -ray irradiation. The ESR signals can be readily seen in Fig. 4, and the weak signals at  $g = 1.9976$  for all samples at different irradiation doses might correspond to radiation-induced defects. For the EPDM, wide peaks are clearly observed in the ESR curve when the irradiation dose reaches 75 kGy, suggesting the generation of irradiation-induced radicals. As the irradiation dose increases to 225 kGy, the intensity of the free-radical signals in the ESR curve of the EPDM decreases slightly, suggesting that the concentration of radicals is reduced mainly due to the recombination reactions between radicals, although new radicals are also formed with increasing irradiation dose. When the irradiation dose reaches 450 kGy, the peaks in the ESR curve of the EPDM become weak; this is because most of the radicals combine with each other to yield nonradical products<sup>41–44</sup>.

Different from the unmodified EPDM, the intensity of the free-radical signals in the ESR curve of the EPDM/1DIP system is very weak at each dose, indicating that DIP has an excellent ability to control the free radicals inside the EPDM during  $\gamma$ -ray irradiation. Taking consideration of the DIP structure, the S–S bond in DIP might break under  $\gamma$ -ray irradiation, and a covalent bond between DIP and the EPDM would form via the reaction between the DIP radicals and the EPDM macroradicals, which is beneficial for

scavenging the EPDM macroradicals at a low irradiation dose. Additionally, when the irradiation dose increases, the xanthate groups in the EPDM chain can react with the radicals and control them; thus, uncontrollable radical-induced chain reactions are significantly inhibited, and the radical concentration in the EPDM is significantly reduced. Moreover, DIP can regenerate via reversible chain transfer; hence, the introduction of DIP into the EPDM can result in a very low concentration of radicals inside the EPDM during  $\gamma$ -ray irradiation.

### Stress relaxation measurements

To investigate whether the introduction of DIP can lead to the formation of controlled architectures and improve the stability of the EPDM microstructure during irradiation, the stress relaxation behavior of the samples was investigated since  $\gamma$ -ray irradiation can significantly change the chain structure of the EPDM, which in turn would have a strong impact on the relaxation behavior of the EPDM chain. Figure 5 shows the stress relaxation curve of the irradiated EPDM samples. In this experiment, a temperature of 180 °C was chosen because high temperatures confer a high mobility to the network chains and thus speed up the stress decay; moreover, high temperatures can accelerate chemical reactions, e.g., oxidative chain scission and crosslinking; thus, the effects of DIP on the structural stabilization of the EPDM might be more clearly observed at high temperatures<sup>45,46</sup>. As can be seen in the figure, the stress relaxation rate of the additive-free EPDM first decreases because of the formation of the crosslinked network in the matrixes; however, as the irradiation dose exceeds 150 kGy, the stress relaxation rate increases, and the relaxation time is reduced. Although the gel content results revealed that the crosslinking degree of the additive-free EPDM increases monotonically with increasing irradiation dose, the excessive crosslinked network formed in the EPDM matrixes when the irradiation dose

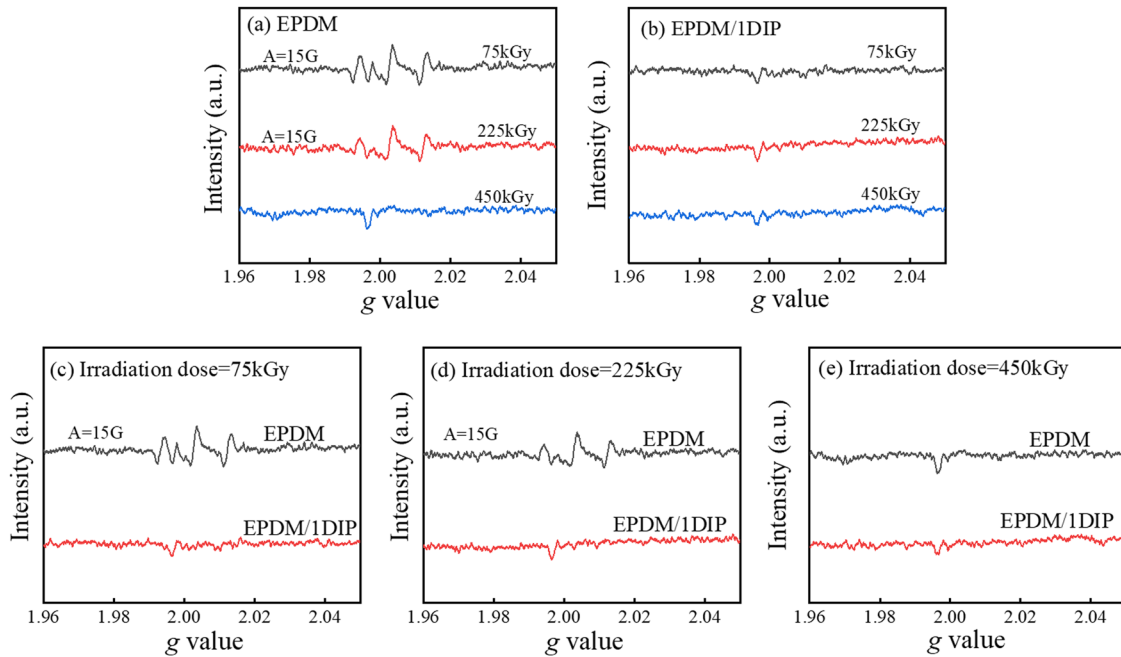


**Fig. 4** ESR curves of the EPDM and EPDM/1DIP blend at different  $\gamma$ -irradiation doses. **a** ESR curves of the EPDM at the indicated irradiation doses, **b** ESR curves of the EPDM/1DIP blend at the indicated irradiation dose; **c** ESR curves of the EPDM and EPDM/1DIP blend at an irradiation dose of 75 kGy; **d** ESR curves of the EPDM and EPDM/1DIP blend at an irradiation dose of 225 kGy; **e** ESR curves of the EPDM and EPDM/1DIP blend at an irradiation dose of 450 kGy.

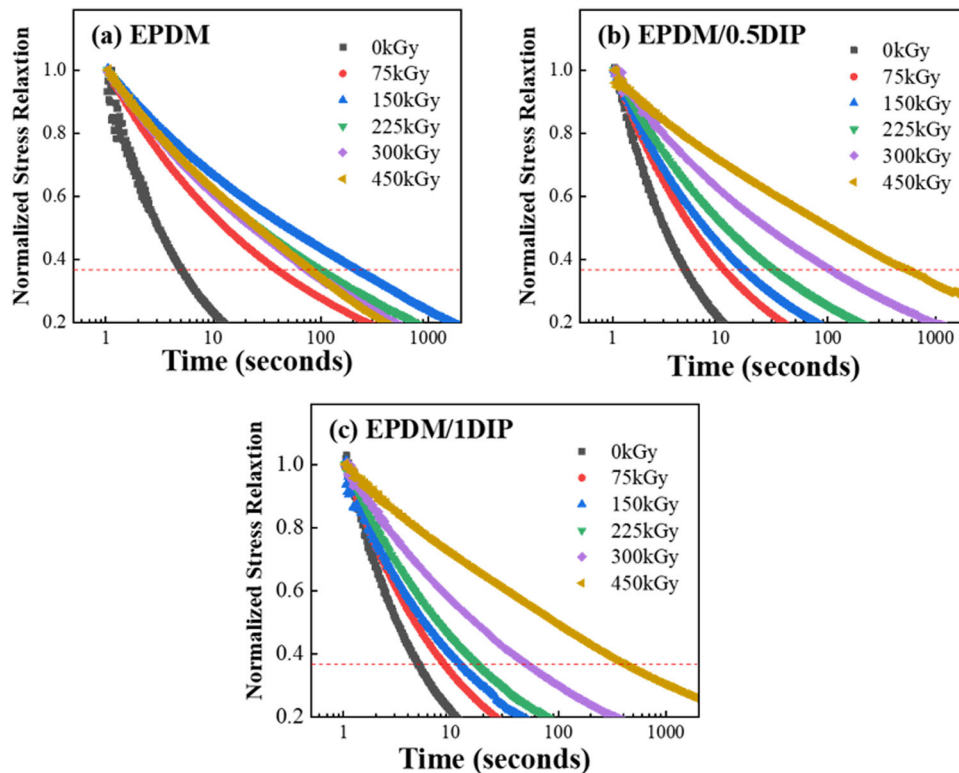


**Fig. 5** Stress relaxation curves of the EPDM and EPDM blends at different  $\gamma$ -irradiation doses measured in air at 180 °C. **a** EPDM, **b** EPDM/0.5DIP blend, **c** EPDM/1DIP blend.

exceeds 300 kGy causes the EPDM to relax more rapidly. Furthermore, the broken chains due to  $\gamma$ -ray irradiation and the uncontrolled radical reactions inside the crosslinked network can also accelerate the stress relaxation of the EPDM<sup>40,47</sup>. For the

EPDM/DIP system, the stress relaxation time increases monotonically with increasing irradiation dose, suggesting that the crosslinked network in the EPDM/DIP blend is stable and is not significantly damaged by  $\gamma$ -ray irradiation.

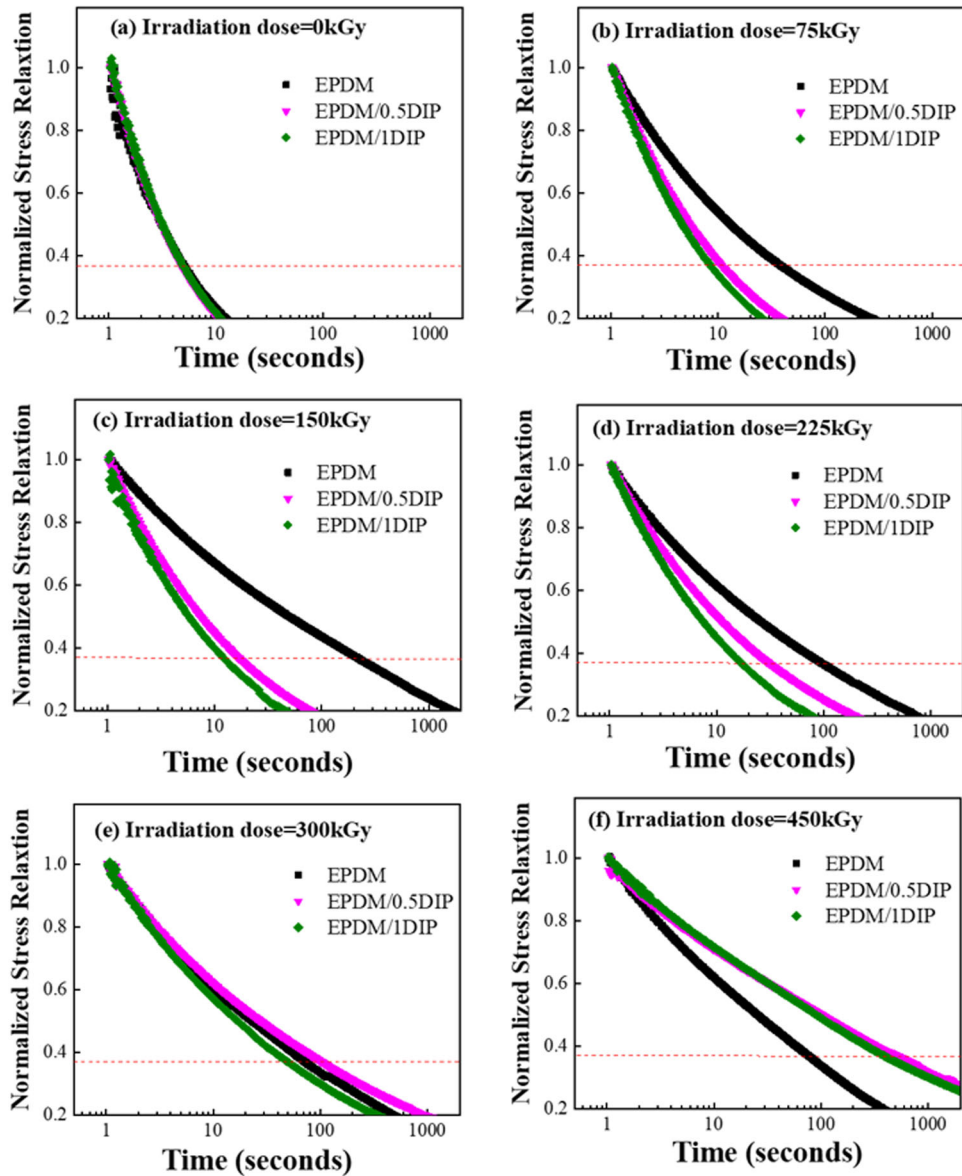


**Fig. 6** Stress relaxation curves of the samples with different blend compositions at different  $\gamma$ -irradiation doses measured in air at 180 °C. **a** 0 kGy, **b** 75 kGy, **c** 150 kGy, **d** 225 kGy, **e** 300 kGy, **f** 450 kGy.

In order to further confirm the protective effect of DIP on the EPDM microstructures, the stress relaxation curves of samples with different blend compositions at specific irradiation doses are presented in Fig. 6. The stress due to deformation can be easily released at high temperatures for the unirradiated EPDM and the EPDM/DIP blends because of the lack of crosslinking. When the irradiation dose reaches 75 kGy, the stress relaxation time increases for all samples owing to the formation of a crosslinked network. The irradiated EPDM/DIP systems exhibit shorter relaxation times than the irradiated additive-free EPDM; this is because DIP can effectively control the radical reactions inside EPDM during irradiation. Thus, the radicals cannot easily react with each other, and the crosslinking degree of the irradiated EPDM/DIP samples is lower than that of the irradiated additive-free EPDM. Furthermore, the EPDM chains in the EPDM/DIP systems can easily move and/or rearrange themselves; thus, the stress of the matrixes is reduced at a higher speed.

Upon further increasing the test time and irradiation dose, the additive-free EPDM is found to still possess a longer relaxation time than the EPDM/DIP systems. However, as the irradiation dose

exceeds 225 kGy, the relaxation of the additive-free EPDM becomes faster, whereas the relaxation time of the EPDM/DIP systems increases monotonically with increasing irradiation dose, and the relaxation of the EPDM/DIP systems becomes slower than that of the additive-free EPDM under a high irradiation dose. As mentioned before, this phenomenon occurs because excessive crosslinking occurs in the EPDM matrixes when the irradiation dose exceeds 300 kGy, which causes the EPDM to relax more rapidly. Additionally, the broken chains due to  $\gamma$ -ray irradiation and the uncontrolled radical reactions inside the crosslinked network can also accelerate the stress relaxation of the EPDM. However, for the EPDM/DIP system, DIP has a considerable capacity to control the radicals inside the EPDM; thus, uncontrolled crosslinking and chain scission of the EPDM chains are inhibited, resulting in the formation of a compact network and the improvement of the structural stability of the EPDM under a high irradiation dose, which leads to a restriction of the EPDM chain mobility in the EPDM/DIP system. According to the comparative mechanical study between the EPDM/DIP and EPDM/antioxidant samples, the mechanical properties of the samples containing

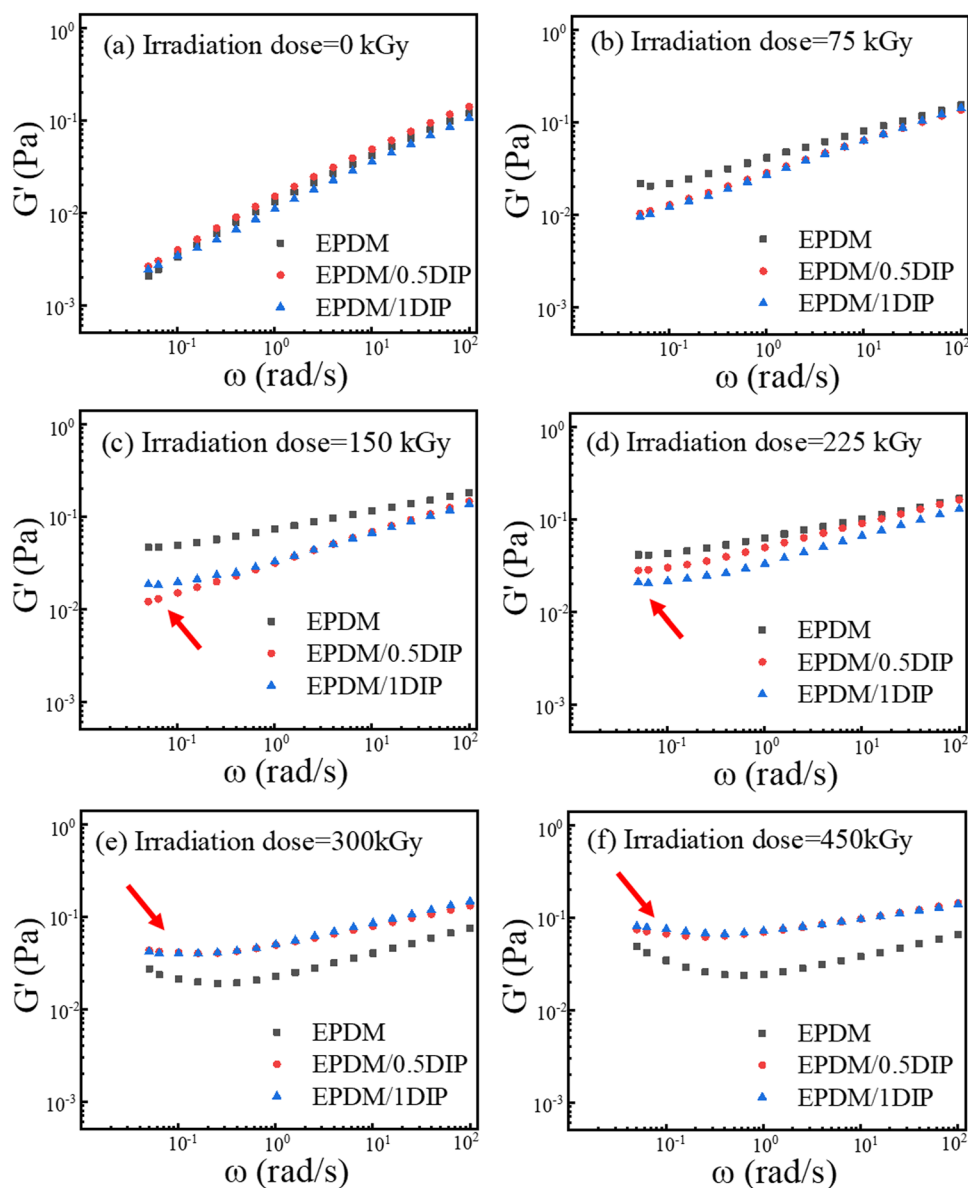


**Fig. 7**  $G'$  of the samples with different blend compositions at different  $\gamma$ -irradiation doses measured in air at 180 °C. **a** 0 kGy, **b** 75 kGy, **c** 150 kGy, **d** 225 kGy, **e** 300 kGy, **f** 450 kGy.

antioxidants are much worse than those of the samples containing DIP under a high irradiation dose (Fig. S3), although the samples containing phenolic antioxidants also possessed a stable crosslink network under high irradiation dose (Figs. S4 and S5). This suggests that the crosslinked network in the EPDM/antioxidant samples might not be well architected compared with that of the EPDM/1DIP sample; thus, the capacity of DIP to control the radical reactions in the EPDM/1DIP blend is further proved.

### Frequency sweep measurements

The plots of the storage modulus ( $G'$ ) versus frequency are shown in Fig. 7 for the EPDM and EPDM/DIP samples at different irradiation doses. For the additive-free EPDM,  $G'$  first increases and then decreases when the irradiation dose exceeds 300 kGy. Although the gel content results indicated that the crosslinking degree of the EPDM increases monotonically with increasing irradiation dose, the damage caused to the crosslinked network of the EPDM by  $\gamma$ -ray irradiation and the uncontrolled radical

reactions leads to a decrease in  $G'$ . Different from the additive-free EPDM, the  $G'$  of the EPDM/DIP systems increases monotonically with increasing irradiation dose; moreover, the EPDM/DIP systems possess a higher  $G'$  than the additive-free EPDM when the irradiation dose exceeds 300 kGy, even though the crosslinking degree of the EPDM/DIP systems is lower than that of the additive-free EPDM according to the gel content results. This suggests that stable crosslinked networks are formed in the EPDM/DIP systems, which is consistent with the stress relaxation results.

### Density functional theory (DFT) calculations

In the pre-equilibrium reaction, the EPDM macroradicals are thought to attack the C=S bonds of DIP. Herein, two potential addition pathways are proposed to investigate the mechanism of the reaction. One is that the macroradicals of the EPDM may attack the C=S bonds of DIP directly. Another is that after the coupling reaction between the EPDM macroradicals and the DIP radical generated from the dissociation of DIP, the EPDM chain containing xanthate groups will be further attacked by other

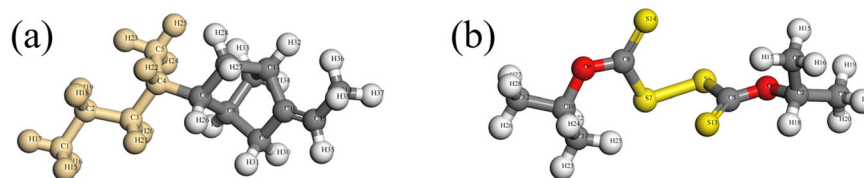


**Fig. 8 Molecular structures. a EPDM and b DIP.**

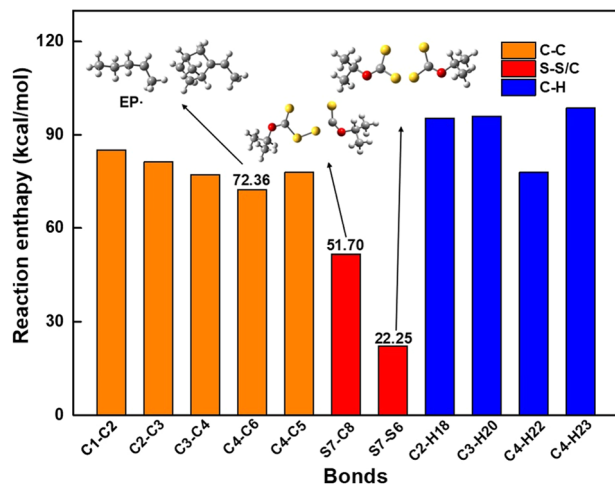


**Fig. 9 Reaction enthalpy of different bonds of EPDM.** Different colors stand for dissociation energies of considered bonds.

EPDM macroradicals to form intermediates, and finally the EPDM macroradicals leave to realize the reversible-addition process.

Under  $\gamma$ -ray irradiation, the EPDM can generate fragments containing radicals that can attack the C=S bonds of DIP. Thus, we consider the reaction between these fragments and DIP to investigate the reaction mechanism. Ethylidene norbornene (ENB) is neglected in the EPDM structure considering its low content in the chain unit (about 0.5%). Figure 8 shows the bonds considered in the EPDM structure (in mustard color) and the DIP structure. To select the bonds that are easy to dissociate, the reaction enthalpy was calculated to determine the bond dissociation energies.

To verify our hypothesis, DFT was used to calculate the addition barrier of two proposed pathways via the Gaussian16 (G16) software. The reaction enthalpy and the reaction barrier were calculated using the UB3LYP method and the 6-31G(d) basis set<sup>48</sup>. Geometry optimizations and frequency analyses were performed to confirm the transition states, and a negative vibrational frequency was observed<sup>49,50</sup>. Figure 9 shows that the reaction enthalpies of different bonds and the bonds between carbon 4 (C4) and carbon 6 (C6) have the lowest reaction enthalpy in EPDM structures (72.36 kcal/mol), which indicates that this site is the easiest to decompose. A corresponding fragment containing the free-radical EP $\cdot$  (labeled in Fig. 9) was used for further analysis.

According to Figs. 10 and 11, the addition barrier of the radical to DIP (44.19 kcal/mol) is bigger than that of the radical to the coupled structure of DIP and EP $\cdot$  (DIPEP, 13.45 kcal/mol), which indicates that the second reaction pathway is the most favorable one. The bond dissociation energies of the S-S and C-S bonds of DIP also support this conclusion. As shown in Fig. 9, the S-S bond (22.25 kcal/mol) can dissociate more easily than the C-S bond (51.70 kcal/mol).

## DISCUSSION

Based on the above results, Figs. 12 and 13 provide a schematic illustration of the mechanisms through which DIP protects the

EPDM. As can be seen in Fig. 12, for the additive-free EPDM, when subjected to  $\gamma$ -ray irradiation, the radicals are formed in the matrixes, and then uncontrolled crosslinking and chain scission occur, which leads to the uncontrolled evolution of the EPDM, and an irregular structure is formed inside the EPDM matrixes. Furthermore, the microstructure of the additive-free EPDM is also easily broken by the  $\gamma$ -ray irradiation because of the uncontrolled radical reactions; thus, the mechanical properties and structural stability of the additive-free EPDM are significantly degraded under a high irradiation dose.

For the EPDM/DIP systems, when subjected to  $\gamma$ -ray irradiation, the S-S bond in DIP breaks, and a covalent bond between DIP and the EPDM is formed via the reaction between the DIP radicals and the EPDM macroradicals. Furthermore, the EPDM macroradicals are scavenged. As the irradiation dose increases, the xanthate groups inside the EPDM matrixes can start to control the radicals. Thus, uncontrollable radical-induced chain reactions are significantly inhibited, and the radical concentration in the EPDM is considerably reduced. Moreover, the xanthate groups can regenerate via reversible chain transfer, which enables the long-term regulation of the radical reactions in the EPDM matrixes. Hence, the introduction of DIP can result in a very low concentration of radicals inside the EPDM during  $\gamma$ -ray irradiation. Due to the ability of DIP to control the radical reactions, the structural evolution of the EPDM is well controlled. Thus, the EPDM possesses excellent stability and mechanical properties under high-dose  $\gamma$ -ray irradiation.

Figure 13 illustrates a simplified reaction scheme for the reactions occurring in the EPDM/DIP systems under  $\gamma$ -ray irradiation, which can correspond to the process of the reversible control of radicals shown in Fig. 12.

In summary, we demonstrated that DIP can control the radical reactions in the EPDM, which is beneficial for avoiding undesirable structural evolution and realizing the long-term stability of the EPDM under  $\gamma$ -ray irradiation. When the irradiation dose reaches 450 kGy, the retention rate of the elongation at break of the EPDM/1DIP system remains about 90%, and its tensile strength increases to nearly 160%, while the retention rate of the elongation at break and the tensile strength of the EPDM remain only about 33% and 70%, respectively, after irradiating with the same dose. On the other hand, the thermal stability of the EPDM decreases considerably after irradiation and is found to be dose dependent. However, the thermal decomposition temperature of the EPDM containing DIP remains basically unchanged with increasing irradiation dose, suggesting that DIP can substantially improve the structural stability of the EPDM. Furthermore, the oxidation resistance of the EPDM is also enhanced owing to the addition of DIP. The ESR studies revealed that DIP can effectively control the radical reactions inside the EPDM matrixes during  $\gamma$ -ray irradiation. The rheology results showed that the structural evolution of the EPDM can be well controlled under  $\gamma$ -ray irradiation owing to the presence of DIP in the EPDM matrixes even at a high irradiation dose, while the structural evolution of the EPDM without DIP is random. The stress relaxation rate of the EPDM/DIP systems at high temperature is much lower than that of the unmodified EPDM at an irradiation dose of 450 kGy because of the compact and stable crosslinked network in the EPDM/DIP systems, although the crosslinking degree of the EPDM/DIP



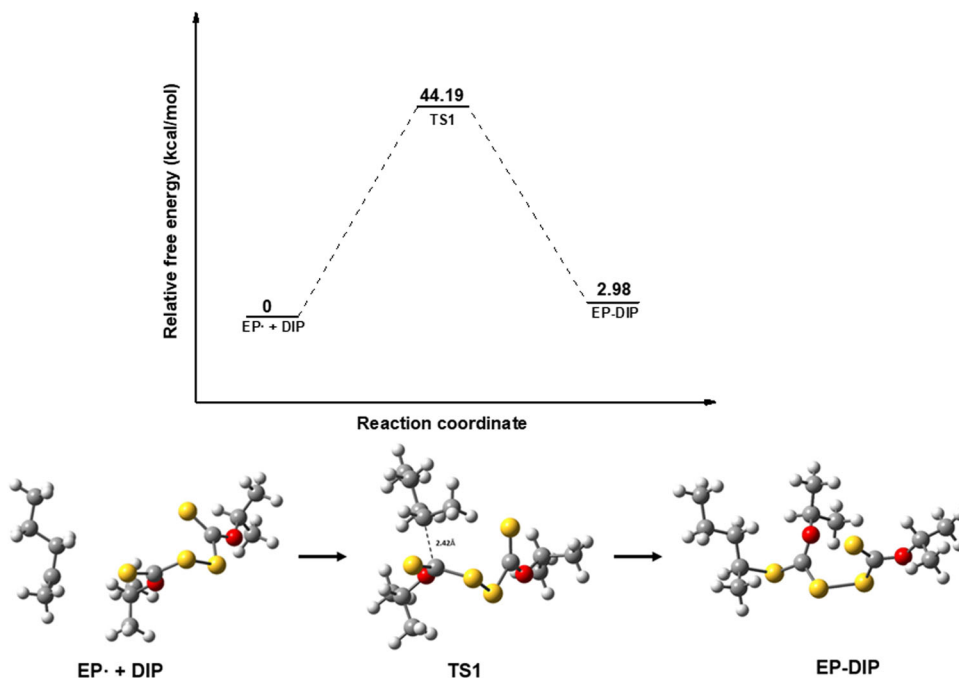


**Fig. 10 Energy profiles and reaction process.** The addition reaction of the first proposed pathway.

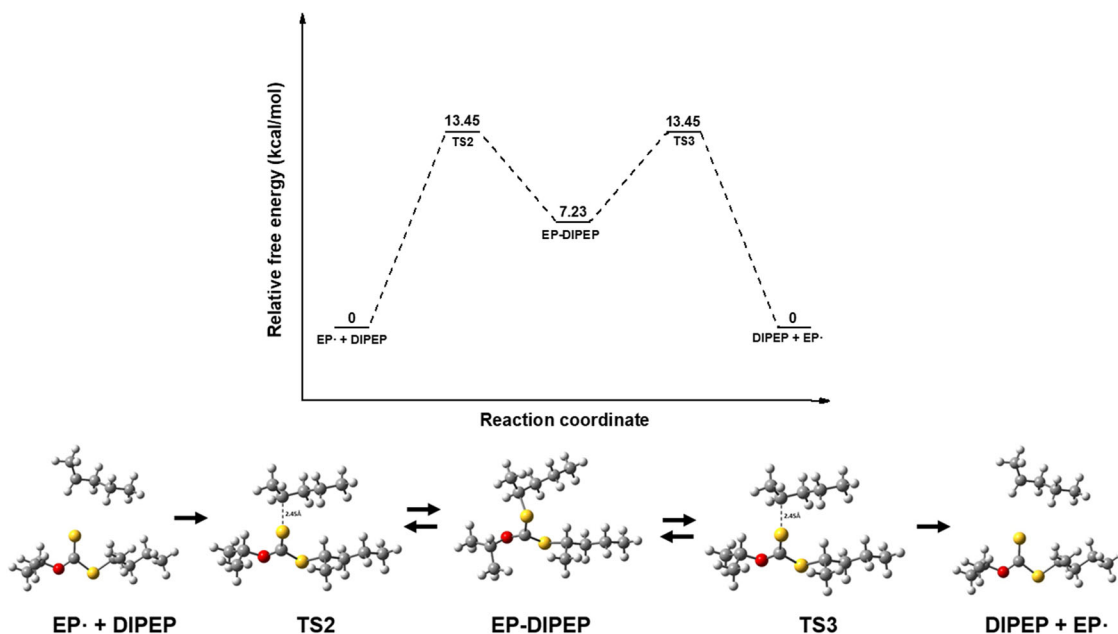


**Fig. 11 Energy profiles and reaction process.** The addition reaction of the second proposed pathway.

systems is much lower than that of the EPDM without DIP at the mentioned dose. Taking into account the DIP structure, it is proposed that when subjected to  $\gamma$ -ray irradiation, the S–S bond in DIP breaks, and covalent bonds between DIP and the EPDM are formed via the reaction between the DIP radicals and the EPDM macroradicals. Then, a relatively unstable activated intermediate radical is formed after the reaction between the xanthates in the EPDM chains and the EPDM macroradicals or chain radicals, and dissociation of the intermediate radical leads to the regeneration of the xanthate groups and the EPDM chain radicals. This enables the realization of the long-term stability and controllable structural

evolution of the EPDM due to abovementioned reversible chain transfer reaction between the EPDM chain containing the xanthate groups and the EPDM chain radicals under  $\gamma$ -ray irradiation. The DFT calculations are consistent with the proposed mechanism.

This work demonstrates that introducing compounds containing groups that have the ability to control the radical reactions is a new method to control the radical reactions inside the EPDM and prolong the service life of the EPDM under  $\gamma$ -ray irradiation. This might provide a universal and effective strategy for other polymers operating in harsh environments.

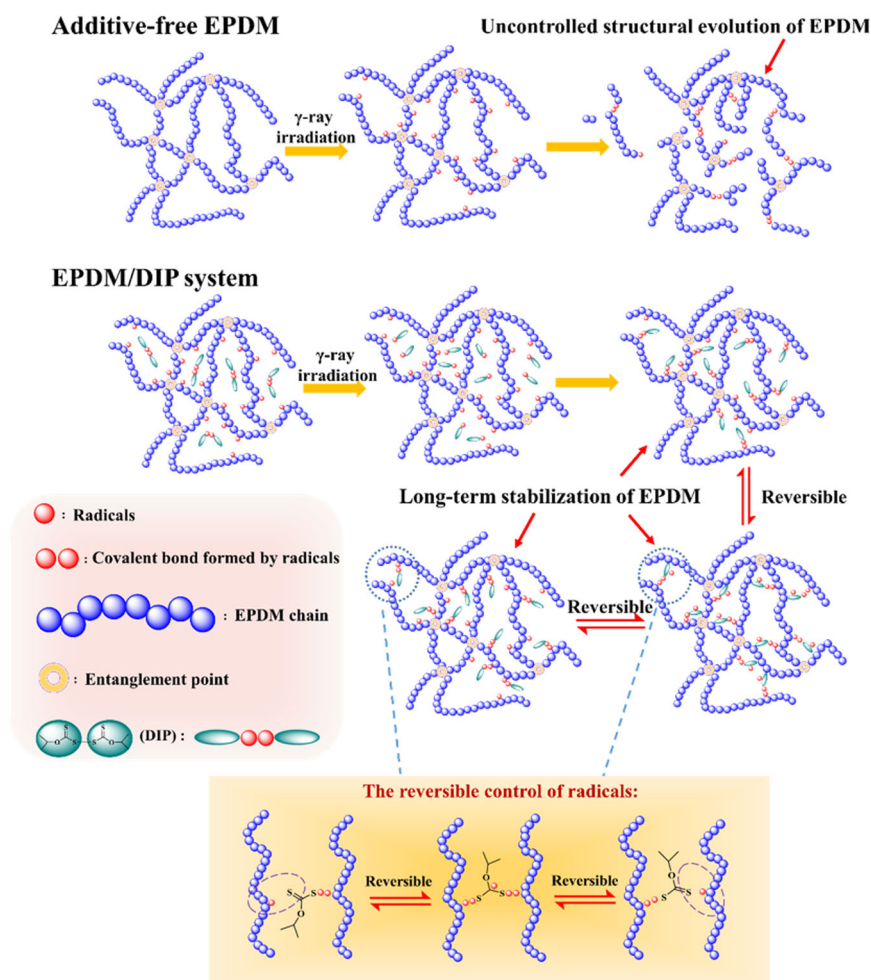


**Fig. 12 Schematic illustration of the mechanisms through which DIP protects the EPDM during irradiation.** Controllable structural evolution of EPDM under irradiation owing to the presence of DIP in the EPDM matrices.

## METHODS

### Materials preparation

The EPDM, NORDEL IP 3722P grade with 71% ethylene content, 0.5% ENB, Mooney viscosity, ML 1 + 4 at 125 °C (ASTM D1646) 18 and density of 0.87 g/mL, was purchased from Dow Chemical. Isopropylxanthic disulfide (DIP, purity > 99%) was purchased from Tianjin Xi'ensi Biochemical Technology Co., Ltd (Tianjin, China). DIP was recrystallized twice from hexane before use, and the DIP structure is shown in Fig. 14.

The additive-free EPDM and the EPDM/DIP blends were prepared using an open two-roll mill at an operating temperature of 100 °C; the total milling time was 10 min. Afterward, the EPDM and the blends were hot-pressed into 1-mm-thick samples at 100 °C and 5 MPa under vacuum. The compositions of the samples are listed in Table 2.

### Irradiation conditions

The samples were irradiated in air at ambient conditions with a  $^{60}\text{Co}$   $\gamma$  source at the University of Science and Technology of China, Hefei, China, at an average dose rate of approximately 3 kGy/h. The total dose was in the range from 0 to 450 kGy.

### Characterizations

The TGA tests of the unirradiated and irradiated EPDM samples were performed in  $\text{N}_2$  atmosphere in a temperature range from

40 °C to 600 °C at a heating rate of 10 °C/min using a TA Q500 instrument. The sample includes both the surface and the internal part of the EPDM.

The surface chemical composition of the unirradiated and irradiated EPDM samples was analyzed using a Nicolet iS5 FT-IR spectrometer (Thermo Fisher Scientific, USA). The ATR FT-IR spectra contain the averages of 32 scans recorded at a resolution of  $2\text{ cm}^{-1}$  in the range from 4000 to  $500\text{ cm}^{-1}$ .

The gel fraction of the unirradiated and irradiated EPDM samples was measured by dissolving the samples in boiling toluene for 24 h and subsequently by drying them in a vacuum oven for several days. The gel fraction was calculated by dividing the remaining mass by the original mass of the polymer.

A Series 3360 universal testing machine (Instron, MA, USA) was used to evaluate the tensile properties of the nonirradiated and irradiated EPDM samples according to the ASTM D standard. The specimens were punched out of the compression-molded sheets into a dumbbell shape. Dumbbell specimens with a length of 35 mm, a thickness of 1 mm, and a narrow section width of 2 mm were used for the test at a crosshead speed of 200 mm/s. Five identical measurements were conducted for each sample.

The room-temperature ESR spectra of the unirradiated and irradiated EPDM samples were obtained using a JEOL JES-FA200 ESR spectrometer at a frequency of 9.086 GHz and in a magnetic field range of 316.5–331.5 mT. The signal intensity was normalized by the sample mass to compensate for possible mass-caused errors.

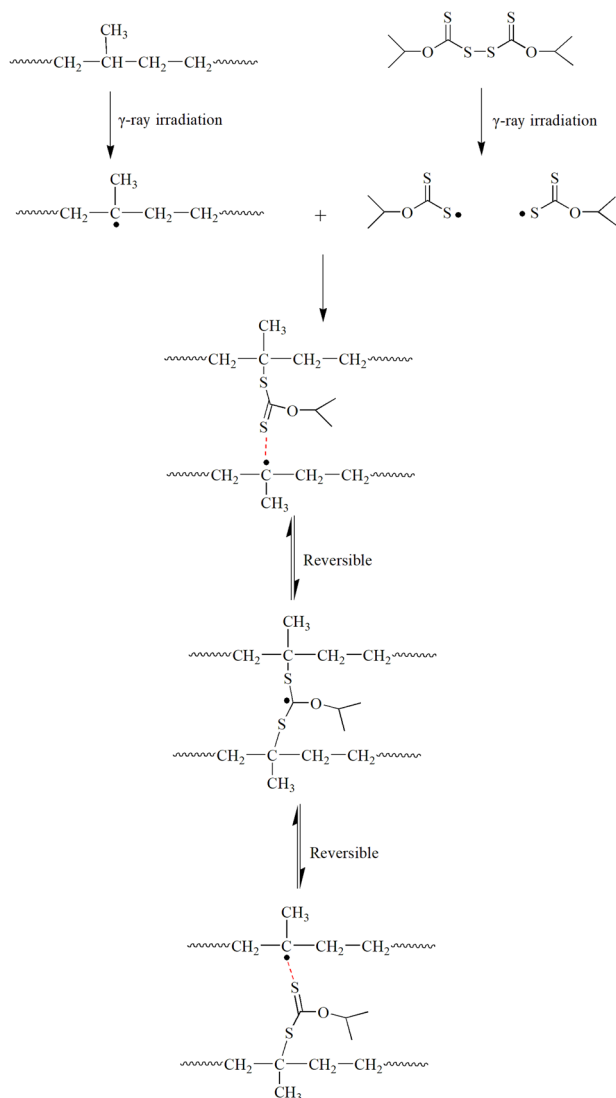


**Fig. 13** Simplified reaction scheme for the reactions occurring in the EPDM/DIP systems under  $\gamma$ -ray irradiation. This Simplified reaction scheme can correspond to the process of the reversible control of radicals shown in Fig. 12.

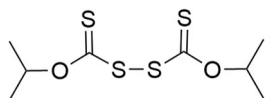


**Fig. 14** Typical DIP structure. The compound that contains the xanthate group.

**Table 2.** Components of the studied EPDM and EPDM/DIP blends.

Sample code	EPDM (w/w %)	DIP (w/w %)
EPDM	100.0	–
EPDM/0.5DIP	99.5	0.5
EPDM/1DIP	99.0	1.0

The stress relaxation dynamics of the unirradiated and irradiated EPDM samples were measured under a strain of 3% and at a temperature of 180 °C using a rheometer (DHR-1, TA Instruments, USA) and 8-mm parallel plates. The samples were

kept at 180 °C for 5 min for thermal equilibration before starting the measurements.

The dynamic frequency sweep measurements were carried out in the linear viscoelastic region in a frequency range of 0.05–100 rad/s, at a strain amplitude of 3% at 180 °C using a rheometer (DHR-1, TA Instruments, USA) and 8-mm parallel plates. The samples were kept for 5 min at 180 °C for thermal equilibration before starting the measurements.

## DATA AVAILABILITY

The data that support the findings of this study are available from the corresponding author upon reasonable request.

Received: 29 October 2022; Accepted: 21 February 2023;  
Published online: 11 March 2023

## REFERENCES

- Song, J. et al. Durable radiative cooling against environmental aging. *Nat. Commun.* **13**, 1–12 (2022).
- Xu, C., Kohler, T. A., Lenton, T. M., Svenning, J. C. & Scheffer, M. Future of the human climate niche. *Proc. Natl Acad. Sci. USA* **117**, 11350–11355 (2020).
- Buongiorno, J., Corradini, M., Parsons, J. & Petti, D. Nuclear energy in a carbon-constrained world: Big challenges and big opportunities. *IEEE Power Energy M.* **17**, 69–77 (2019).
- Alam, F., Sarkar, R. & Chowdhury, H. Nuclear power plants in emerging economies and human resource development: a review. *Energy Procedia* **160**, 3–10 (2019).
- Mazzucchi, N. Nuclear power can help the democratic world achieve energy independence. *Nature* **606**, 841–841 (2022).
- Mo, Y. M., Gong, Y. & Yang, Z. G. Failure analysis on the O-ring of radial thrust bearing room of main pump in a nuclear power plant. *Eng. Fail. Anal.* **115**, 104673 (2020).
- Audouin, L., Langlois, V., Verdu, J. & De Bruijn, J. C. M. Role of oxygen diffusion in polymer ageing: kinetic and mechanical aspects. *J. Mater. Sci.* **29**, 569–583 (1994).
- Seguchi, T., Tamura, K., Shimada, A., Sugimoto, M. & Kudoh, H. Mechanism of antioxidant interaction on polymer oxidation by thermal and radiation ageing. *Radiat. Phys. Chem.* **81**, 1747–1751 (2012).
- Watanabe, R. et al. Polypropylene-based nanocomposite with enhanced aging stability by surface grafting of Silica Nanofillers with a silane coupling agent containing an antioxidant. *ACS Omega* **5**, 12431–12439 (2020).
- Seguchi, T., Tamura, K., Ohshima, T., Shimada, A. & Kudoh, H. Degradation mechanisms of cable insulation materials during radiation–thermal ageing in radiation environment. *Radiat. Phys. Chem.* **80**, 268–273 (2011).
- Kang, J., Tok, J. B. H. & Bao, Z. Self-healing soft electronics. *Nat. Electron.* **2**, 144–150 (2019).
- Scott, G. & Yusoff, M. F. Mechanisms of antioxidant action: autolytic functions. *Eur. Polym. J.* **16**, 497–501 (1980).
- Farzaliev, V. M., Fernando, W. S. E. & Scott, G. Mechanisms of antioxidant action: auto-synergistic behaviour of sulphur-containing phenols. *Eur. Polym. J.* **14**, 785–788 (1978).
- Pospíšil, J. Mechanistic action of phenolic antioxidants in polymers—a review. *Polym. Degrad. Stab.* **20**, 181–202 (1988).
- Zou, Y., He, J., Tang, Z., Zhu, L. & Liu, F. Structural and mechanical properties of styrene–butadiene rubber/silica composites with an interface modified in-situ using a novel hindered phenol antioxidant and its samarium complex. *Compos. Sci. Technol.* **188**, 107984 (2020).
- Nicolas, C. et al. ROMP of novel hindered phenol-functionalized norbornenes and preliminary evaluation as stabilizing agents. *Polym. Degrad. Stab.* **186**, 109522 (2021).
- Rivatton, A., Cambon, S. & Gardette, J. L. Radiochemical ageing of ethylene–propylene–diene elastomers. 4. Evaluation of some anti-oxidants. *Polym. Degrad. Stab.* **91**, 136–143 (2006).
- Moad, G., Rizzardo, E. & Thang, S. H. RAFT polymerization and some of its applications. *Chem. Asian J.* **8**, 1634–1644 (2013).
- Perrier, S. 50th Anniversary perspective: RAFT polymerization—a user guide. *Macromolecules* **50**, 7433–7447 (2017).
- Nothling, M. D. et al. Progress and perspectives beyond traditional RAFT polymerization. *Adv. Sci.* **7**, 2001656 (2020).
- Barner-Kowollik, C. et al. Mechanism and kinetics of dithiobenzoate-mediated RAFT polymerization. I. The current situation. *J. Polym. Sci. Part A Polym. Chem.* **44**, 5809–5831 (2006).

22. Boyer, C., Stenzel, M. H. & Davis, T. P. Building nanostructures using RAFT polymerization. *J. Polym. Sci. Part A Polym. Chem.* **49**, 551–595 (2011).
23. Hill, M. R., Carmean, R. N. & Sumerlin, B. S. Expanding the scope of RAFT polymerization: recent advances and new horizons. *Macromolecules* **48**, 5459–5469 (2015).
24. Destarac, M. Controlled radical polymerization: industrial stakes, obstacles and achievements. *Macromol. React. Eng.* **4**, 165–179 (2010).
25. Barsbay, M. & Güven, O. Nanostructuring of polymers by controlling of ionizing radiation-induced free radical polymerization, copolymerization, grafting and crosslinking by RAFT mechanism. *Radiat. Phys. Chem.* **169**, 107816 (2020).
26. Sütökin, S. D. & Güven, O. Radiation-induced controlled polymerization of acrylic acid by RAFT and RAFT-MADIX methods in protic solvents. *Radiat. Phys. Chem.* **142**, 82–87 (2018).
27. Quinn, J. F., Davis, T. P., Barner, L. & Barner-Kowollik, C. The application of ionizing radiation in reversible addition–fragmentation chain transfer (RAFT) polymerization: renaissance of a key synthetic and kinetic tool. *Polymer* **48**, 6467–6480 (2007).
28. Millard, P. E. et al. Synthesis of water-soluble homo- and block-copolymers by RAFT polymerization under  $\gamma$ -irradiation in aqueous media. *Polymer* **51**, 4319–4328 (2010).
29. Keddie, D. J., Moad, G., Rizzardo, E. & Thang, S. H. RAFT agent design and synthesis. *Macromolecules* **45**, 5321–5342 (2012).
30. Li, C., He, J., Zhou, Y., Gu, Y. & Yang, Y. Radical-induced oxidation of RAFT agents—a kinetic study. *J. Polym. Sci. Part A Polym. Chem.* **49**, 1351–1360 (2011).
31. Šarac, T., Quiévy, N., Gusarov, A. & Konstantinović, M. J. Influence of  $\gamma$ -irradiation and temperature on the mechanical properties of EPDM cable insulation. *Radiat. Phys. Chem.* **125**, 151–155 (2016).
32. Le Lay, F. Study on the lifetime of EPDM seals in nuclear-powered vessels. *Radiat. Phys. Chem.* **84**, 210–217 (2013).
33. Rivaton, A., Cambon, S. & Gardette, J. L. Radiochemical ageing of EPDM elastomers. *Nucl. Instr. Methods B* **3**, 343–356 (2005).
34. Planes, E., Chazeau, L., Vigier, G., Fournier, J. & Stevenson-Royaud, I. Influence of fillers on mechanical properties of ATH filled EPDM during ageing by gamma irradiation. *Polym. Degrad. Stab.* **95**, 1029–1038 (2010).
35. Jandura, P., Riedl, B. & Kokta, B. V. Thermal degradation behavior of cellulose fibers partially esterified with some long chain organic acids. *Polym. Degrad. Stab.* **70**, 387–394 (2000).
36. Zhou, W., Yang, H., Guo, X. & Lu, J. Thermal degradation behaviors of some branched and linear polysiloxanes. *Polym. Degrad. Stab.* **91**, 1471–1475 (2006).
37. Yan, P. et al. Inverse vulcanized polymers with shape memory, enhanced mechanical properties, and vitrimer behavior. *Angew. Chem. Int. Ed.* **59**, 13371–13378 (2020).
38. Zaharescu, T. et al. Prevention of degradation of  $\gamma$ -irradiated EPDM using phenolic antioxidants. *Chem. Pap.* **70**, 495–504 (2016).
39. El-Nemr, K. F., Khaffaga, M. M., Saleh, S. N. & Zahran, M. K. Physico-chemical and spectroscopic properties of gamma irradiated ethylene propylene diene monomer rubber/vermiculite clay/maleic anhydride nanocomposites. *Polym. Compos.* **39**, 2469–2478 (2018).
40. Planes, E., Chazeau, L., Vigier, G. & Fournier, J. Evolution of EPDM networks aged by gamma irradiation—Consequences on the mechanical properties. *Polymer* **50**, 4028–4038 (2009).
41. Bracco, P., Costa, L., Luda, M. P. & Billingham, N. A review of experimental studies of the role of free-radicals in polyethylene oxidation. *Polym. Degrad. Stab.* **155**, 67–83 (2018).
42. Liu, S. et al. Study on the post-irradiation oxidation of polyethylenes using EPR and FTIR technique. *Polym. Degrad. Stab.* **196**, 109846 (2022).
43. Zachary, M. et al. EPR study of persistent free radicals in cross-linked EPDM rubbers. *Eur. Polym. J.* **44**, 2099–2107 (2008).
44. Passaglia, E., Coiai, S. & Augier, S. Control of macromolecular architecture during the reactive functionalization in the melt of olefin polymers. *Prog. Polym. Sci.* **34**, 911–947 (2009).
45. Zhao, J., Yang, R., Iervolino, R., Vorst, B. & Barbera, S. The effect of thermo-oxidation on the continuous stress relaxation behavior of nitrile rubber. *Polym. Degrad. Stab.* **115**, 32–37 (2015).
46. Lou, W., Xie, C. & Guan, X. Coupled effects of temperature and compressive strain on aging of silicone rubber foam. *Polym. Degrad. Stab.* **195**, 109810 (2022).
47. Kittur, M. I., Andriyana, A., Ang, B. C., Ch'ng, S. Y. & Verron, E. Inelastic response of thermo-oxidatively aged carbon black filled polychloroprene rubber. Part 1: viscoelasticity Inelastic response of thermo-oxidatively aged carbon black filled polychloroprene rubber. Part II: Mullins effect. *Polym. Degrad. Stab.* **204**, 110118 (2022).
48. Parr, R. G. & Yang, W. *Density-Functional Theory of Atoms and Molecules* (Oxford University Press, Oxford, 1989).
49. Coote, M. L. The kinetics of addition and fragmentation in reversible addition fragmentation chain transfer polymerization: An ab initio study. *J. Phys. Chem. A* **109**, 1230–1239 (2005).
50. Izgorodina, E. I. & Coote, M. L. Reliable low-cost theoretical procedures for studying addition-fragmentation in RAFT polymerization. *J. Phys. Chem. A* **110**, 2486–2492 (2006).

## ACKNOWLEDGEMENTS

This research was supported by the National Natural Science Foundation of China (No. 51673056), Major scientific and technological achievements engineering research and development project of Anhui province (201903c08020009), School-local government cooperation industries innovation guidance fund (JZ2020YDZJ0333), Platform project of School-local government cooperation industries innovation guidance fund (JZ2020YDZJ0005), School-local government cooperation industries innovation guidance fund project (JZ2019AHD50006). Y.D. acknowledges Prof. Jiafu Chen at Physical and Chemical Science Center of University of Science and Technology of China for the ESR measurements.

## AUTHOR CONTRIBUTIONS

Y.D. designed the research and led the study, Y.Z. designed and produced the samples, all authors conducted the research and analyzed the results; Y.Z. and Y.D. wrote the manuscript and all authors read and edited the manuscript.

## COMPETING INTERESTS

The authors declare no competing interests.

## ADDITIONAL INFORMATION

**Supplementary information** The online version contains supplementary material available at <https://doi.org/10.1038/s41529-023-00334-9>.

**Correspondence** and requests for materials should be addressed to Yunsheng Ding.

**Reprints and permission information** is available at <http://www.nature.com/reprints>

**Publisher's note** Springer Nature remains neutral with regard to jurisdictional claims in published maps and institutional affiliations.



**Open Access** This article is licensed under a Creative Commons Attribution 4.0 International License, which permits use, sharing, adaptation, distribution and reproduction in any medium or format, as long as you give appropriate credit to the original author(s) and the source, provide a link to the Creative Commons license, and indicate if changes were made. The images or other third party material in this article are included in the article's Creative Commons license, unless indicated otherwise in a credit line to the material. If material is not included in the article's Creative Commons license and your intended use is not permitted by statutory regulation or exceeds the permitted use, you will need to obtain permission directly from the copyright holder. To view a copy of this license, visit <http://creativecommons.org/licenses/by/4.0/>.

© The Author(s) 2023